Supporting Information

Zhang et al. 10.1073/pnas.1208787109

SI Results

Resonance Raman Characterization of the $[4Fe\text{-}4S]^{2+}$ Center in Fumarate and Nitrate Reduction. Assignments of the Fe-S stretching modes of the $[Fe_4S_4(SCys)_4]$ center in fumarate and nitrate reduction (FNR) under idealized D_{2d} symmetry have been made based on downshifts on ^{34}S substitution of bridging S atoms and comparison with assignments based on normal mode calculations for the $(Et_4N)_2[Fe_4S_4(SCH_2Ph)_4]$ analog complex and *Clostridium pasteurianum* 8Fe ferredoxin (Table S1).

Resonance Raman Characterization of the Formation of Cysteine Persulfide $[2Fe\text{-}2S]^{2+}$ Clusters in O_2-Exposed $[4Fe\text{-}4S]$-FNR. The effect of GSH and DTT on the formation of the cysteine persulfide-ligated $[2Fe\text{-}2S]^{2+}$ center in FNR by air exposure of $[4Fe\text{-}4S]$-FNR was investigated by measuring resonance Raman spectra in the absence and presence of 3 mM GSH or 8 mM DTT (Fig. S1). The close similarity in the spectra and the presence of the S-S stretching mode of the ligating cysteine persulfides in all three spectra demonstrate that physiological levels of GSH or 8 mM DTT do not prevent O_2-induced formation of cysteine persulfide-ligated $[2Fe\text{-}2S]^{2+}$ centers in FNR.

The time course of O_2-induced $[4Fe\text{-}4S]^{2+}$ to $[2Fe\text{-}2S]^{2+}$ cluster conversion in FNR was monitored by resonance Raman at 457 nm and 488 nm for samples frozen between 30 s and 60 min after exposure to air (Fig. S2). The results indicate that the overwhelming majority of the $[4Fe\text{-}4S]^{2+}$ cluster are degraded within the first 30 s of air exposure. However, the spectra from the resultant cysteine persulfide-ligated $[2Fe\text{-}2S]^{2+}$ cluster continue to undergo subtle changes as the time of air exposure is increased from 30 s to 60 min. These changes are attributed to the initial formation of FNR with primarily one cysteine persulfide-ligated $[2Fe\text{-}2S]^{2+}$ cluster and increasing concentrations of FNR with two cysteine persulfide-ligated $[2Fe\text{-}2S]^{2+}$ clusters as time of air-exposure increases, based on liquid-chromatography electrospray-ionization mass spectrometry (LC-ESI-MS) time-course data and CD estimates of the extent of reversibility in the absence of exogenous sulfide.

The lower resonance enhancement of the $[2Fe\text{-}2S]^{2+}$ cluster Raman spectrum with 488-nm excitation facilitates observation of the Fe_3-(μ_3-S) symmetric stretching mode of a cubane-type $[3Fe\text{-}4S]^{1+}$ cluster at 347 cm^{-1}. This band dominates the spectrum of this type of cluster with 488-nm excitation, as indicated by the resonance Raman spectrum of the well-characterized cubane-type $[3Fe\text{-}4S]^{1+}$ cluster in *Pyrococcus furiosus* ferredoxin (1–3) (Fig. S2). However, the strong resonance enhancement of this band compared with the very weak resonant enhancement of the cysteine persulfide-ligated $[2Fe\text{-}2S]^{2+}$ cluster in FNR indicates that this corresponds to a trace amount of $[3Fe\text{-}4S]^{1+}$ cluster in FNR. Coupled with lack of a significant change in relative intensity of the bands associated with the $[3Fe\text{-}4S]^{1+}$ cluster and cysteine persulfide-ligated $[2Fe\text{-}2S]^{2+}$ cluster with time, this finding suggests that the observed cubane-type $[3Fe\text{-}4S]^{1+}$ cluster is a dead-end product that fails to undergo conversion to the $[2Fe\text{-}2S]^{2+}$ form and is incapable of further interaction with O_2.

UV-Visible Absorption and CD Studies of the $[2Fe\text{-}2S]^{2+}$ to $[4Fe\text{-}4S]^{2+}$ Cluster Conversion in FNR. UV-visible absorption and CD were used to provide a quantitative assessment of the extent of $[2Fe\text{-}2S]^{2+}$ to $[4Fe\text{-}4S]^{2+}$ cluster conversion in FNR under anaerobic conditions. An initial set of experiments was carried out with samples of $[2Fe\text{-}2S]^{2+}$-FNR prepared by exposing $[4Fe\text{-}4S]^{2+}$-FNR to O_2 for 2 min without repurification to remove breakdown products (Fig. S3). No reaction occurred in the absence of DTT, which is presumably required to reductively cleave persulfides, but the conversion to the characteristic absorption and CD spectrum of $[4Fe\text{-}4S]^{2+}$-FNR (4) proceeds rapidly on addition of 3 mM DTT using the Fe^{2+} released during $[4Fe\text{-}4S]^{2+}$ to $[2Fe\text{-}2S]^{2+}$ cluster conversion. The reaction starts to slow down after about 20 min, but after 109 min, addition of an eightfold excess of Fe^{2+} (compared with the initial $[2Fe\text{-}2S]^{2+}$-FNR concentration) results in a small additional increase in intensity of the spectra attributed to $[4Fe\text{-}4S]^{2+}$-FNR. The reaction was complete within 10 min for samples that were treated with 3 mM DTT and an eightfold excess of Fe^{2+} at the start of the reaction, and in both sets of experiments the recovered yield of $[4Fe\text{-}4S]^{2+}$ clusters was ~75%, based on the published absorption and CD extinction coefficients (4).

Parallel experiments after anaerobic removal of cluster degradation products via gel filtration after exposing $[4Fe\text{-}4S]^{2+}$-FNR to O_2 for 2 min are shown in Fig. S4. Little reconversion to $[4Fe\text{-}4S]^{2+}$-FNR was observed during exposure to 3 mM DTT for 50 min. However, rapid reconversion to $[4Fe\text{-}4S]^{2+}$-FNR with a ~63% yield was observed on addition of an eightfold excess of Fe^{2+} (compared with the initial $[2Fe\text{-}2S]^{2+}$-FNR concentration). A slightly higher yield (~70%) was obtained after 10 min of reaction when 3 mM DTT and an eightfold excess of Fe^{2+} were added together at the start of the reaction, suggesting some DTT-induced cluster degradation occurs in the absence of Fe^{2+}. In contrast, no significant $[2Fe\text{-}2S]^{2+}$-FNR to $[4Fe\text{-}4S]^{2+}$-FNR conversion occurred using 3 mM GSH and a eightfold excess of Fe^{2+}. These results clearly demonstrate that up to 70% of the initial $[4Fe\text{-}4S]^{2+}$-FNR can be recovered rapidly (<10 min) from $[2Fe\text{-}2S]^{2+}$-FNR in the absence of exogenous sulfide, but in the presence of a dithiol reagent and a small excess of Fe^{2+}.

SI Materials and Methods

Absorption and CD measurements were made using a Jasco V550 UV-visible spectrophotometer and Jasco J-810 spectropolarimeter, respectively. Raman samples (~2 mM in [4Fe-4S] clusters) were placed onto the sample holder inside the glove box under Ar atmosphere. For the oxygen-exposed samples, the $[4Fe\text{-}4S]^{2+}$ cluster-containing FNR and biotin synthase (BioB) Raman samples were thawed under an Ar atmosphere before being taken outside the glove box and exposed to air for 20 min with gentle mixing using a syringe. Resonance Raman samples were in the form of a 20-μL frozen droplet mounted on the cold finger of an Displex Model CSA-202E closed-cycle refrigerator (Air Products) and resonance Raman spectra were recorded using a Ramanor U1000 scanning spectrometer (Instrument SA) coupled with a Sabre argon ion laser (Coherent), as previously described (5, 6). MS was used to investigate the formation of cysteine persulfides on FNR as a function of time of oxygen exposure. Five-microliter aliquots of FNR (~1 mM in $[4Fe\text{-}4S]^{2+}$ clusters) were exposed to air for time intervals between 0 and 60 min. Immediately after exposure to air, the samples were mixed with 20 μL of a 1% (vol/vol) aqueous solution of formic acid (solvent A) and injected into the LC-ESI-MS. The samples were purified using a BioBasic-4 column, as previously described (7), using solvent A and acetonitrile with 1% formic acid as solvent B, except that both solvents were rigorously degassed before use. The HPLC flow rate was 50 μL/min and samples were injected in 25-μL aliquots into 10% solvent B and solvent B was increased to

95% over 20 min and maintained at 95% for 5 min before reaching 100% using an Applied Biosystems 140B solvent delivery system. The effluent was analyzed using a single quadrupole MS equipped with an ESI source (PE Sciex API I plus) and the mass spectrum was scanned from 700–1600 *m/z*. The reported masses are accurate to ± 0.1%.

1. Conover RC, et al. (1990) Spectroscopic characterization of the novel iron-sulfur cluster in *Pyrococcus furiosus* ferredoxin. *J Biol Chem* 265:8533–8541.
2. Duderstadt RE, Staples CR, Brereton PS, Adams MWW, Johnson MK (1999) Effects of mutations in aspartate 14 on the spectroscopic properties of the $[Fe_3S_4]^{+,0}$ clusters in *Pyrococcus furiosus* ferredoxin. *Biochemistry* 38:10585–10593.
3. Johnson MK, Duderstadt RE, Duin EC (1999) Biological and synthetic $[Fe_3S_4]$ clusters. *Adv Inorg Chem* 47:1–82.
4. Crack JC, et al. (2008) Influence of the environment on the $[4Fe\text{-}4S]^{2+}$ to $[2Fe\text{-}2S]^{2+}$ cluster switch in the transcriptional regulator FNR. *J Am Chem Soc* 130:1749–1758.
5. Drozdzewski PM, Johnson MK (1988) A simple anaerobic cell for low temperature Raman spectroscopy. *Appl Spectrosc* 42:1575–1577.
6. Cosper MM, et al. (2004) Characterization of the cofactor composition of Escherichia coli biotin synthase. *Biochemistry* 43:2007–2021.
7. Smith AD, et al. (2001) Sulfur transfer from IscS to IscU: The first step in iron-sulfur cluster biosynthesis. *J Am Chem Soc* 123:11103–11104.

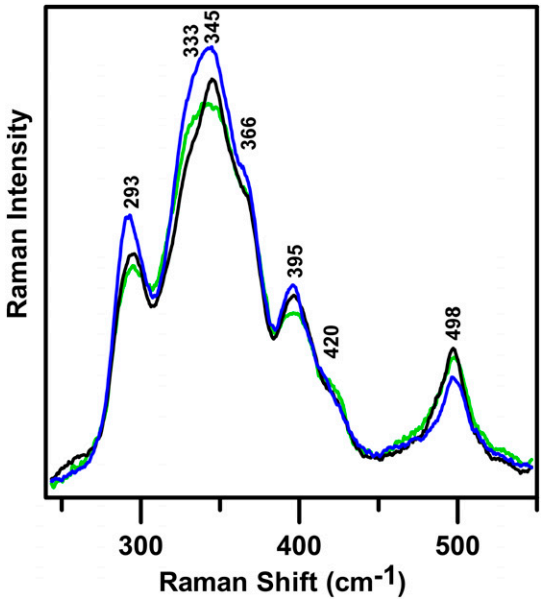

Fig. S1. Comparison of the resonance Raman spectra of air-exposed FNR obtained in the absence (black spectra) and presence of GSH (green spectra) or DTT (blue spectra). The FNR samples were ~2 mM in $[4Fe\text{-}4S]^{2+}$ clusters and were incubated with a final concentration of 3 mM GSH or 8 mM DTT under anaerobic conditions before air exposure for 20 min. The Raman experimental conditions are the same as described in Fig. 2.

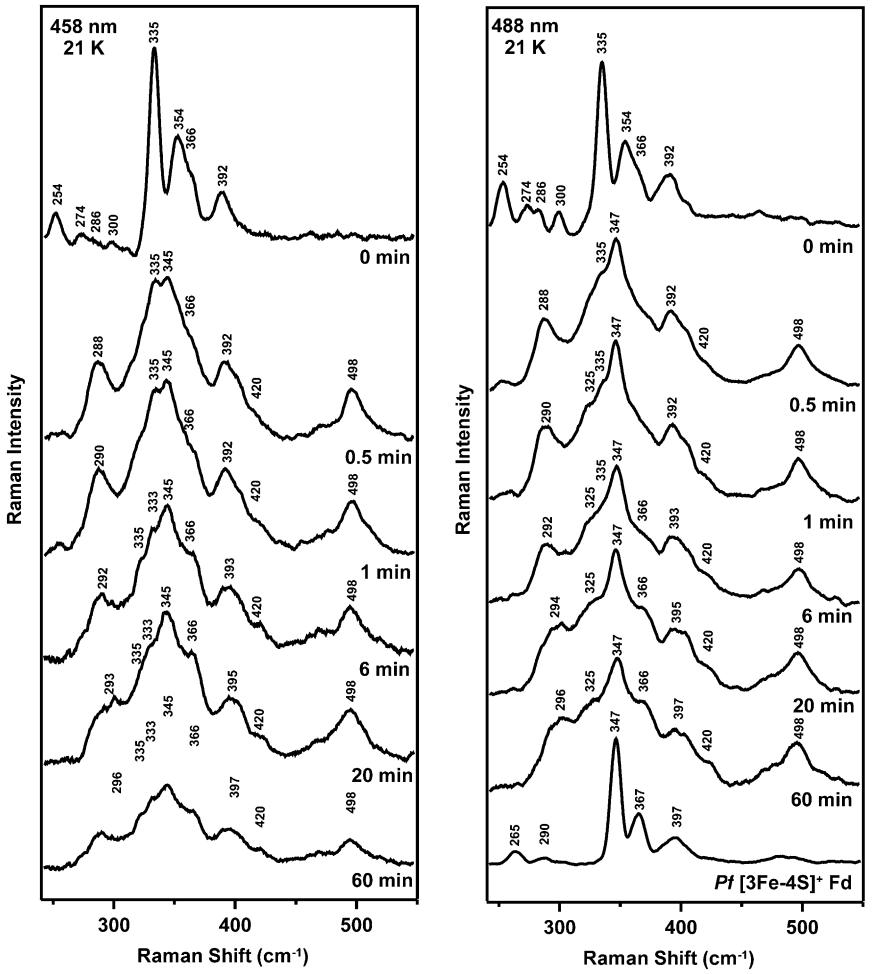

Fig. S2. Time course of the resonance Raman spectrum of FNR after exposure to air (0–60 min). Samples were exposed to air in the absence of DTT or GSH. The resonance Raman experimental conditions are the same as described in Fig. 2 and the excitation wavelengths and sample temperatures are shown on each set of spectra. The resonance Raman spectrum of the $[3Fe\text{-}4S]^{+}$ cluster in *P. furiosus* ferredoxin is shown for comparison with the data collected at 488 nm.

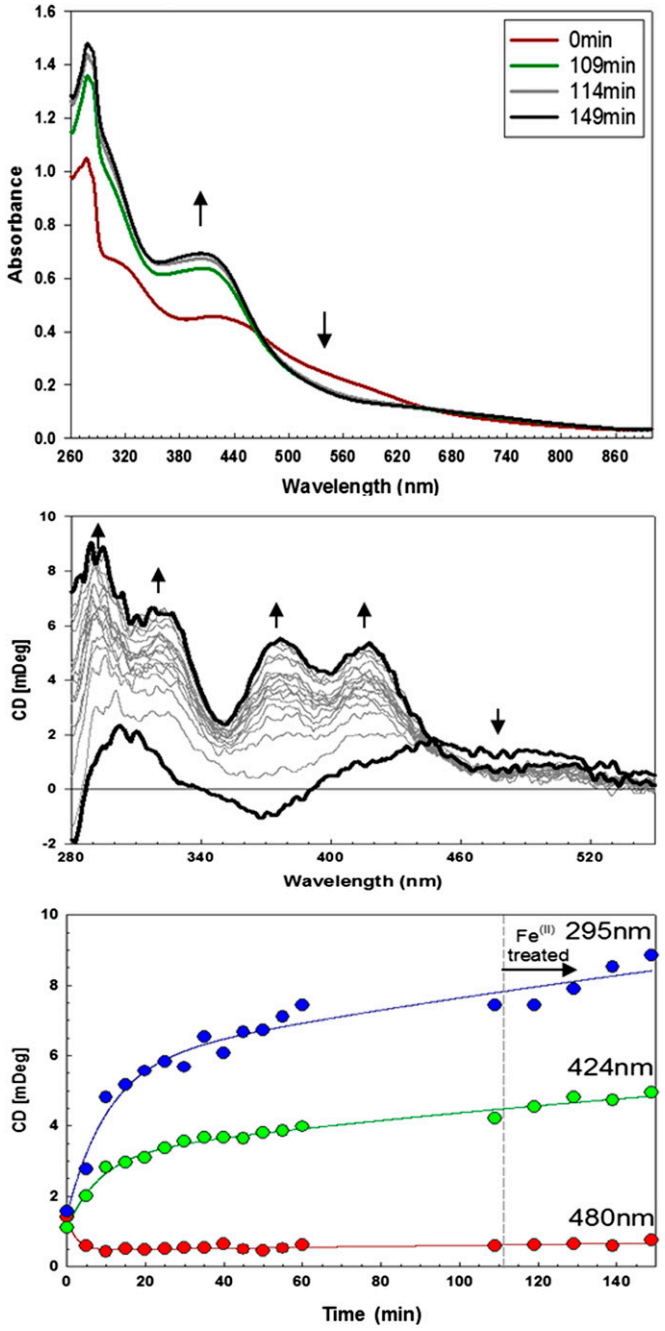

Fig. S3. UV-visible absorption and CD time course of $[2Fe\text{-}2S]^{2+}$ to $[4Fe\text{-}4S]^{2+}$ cluster conversion in FNR without repurification of $[2Fe\text{-}2S]^{2+}$-FNR. Sample of $[2Fe\text{-}2S]^{2+}$-FNR was obtained by exposing $[4Fe\text{-}4S]^{2+}$-FNR to O_2 for 2 min and the concentration of $[2Fe\text{-}2S]^{2+}$ centers in FNR was 57 μM. The samples were treated with 3 mM DTT at 0 min and an eightfold excess of ferrous ammonium sulfate was added after 109 min under anaerobic conditions inside a glove box. (*Top*) Absorption spectra recorded after 0, 109, 114, and149 min; arrows indicate the direction of changes of absorption intensity as a function of time at discrete wavelengths. (*Middle*) CD spectra (gray lines) recorded between 0 and 149 min (bold lines); arrows indicate the direction of change of CD intensity as a function of time at discrete wavelengths. (*Bottom*) Plot of CD intensity at 295, 424, and 480 nm as a function of time.

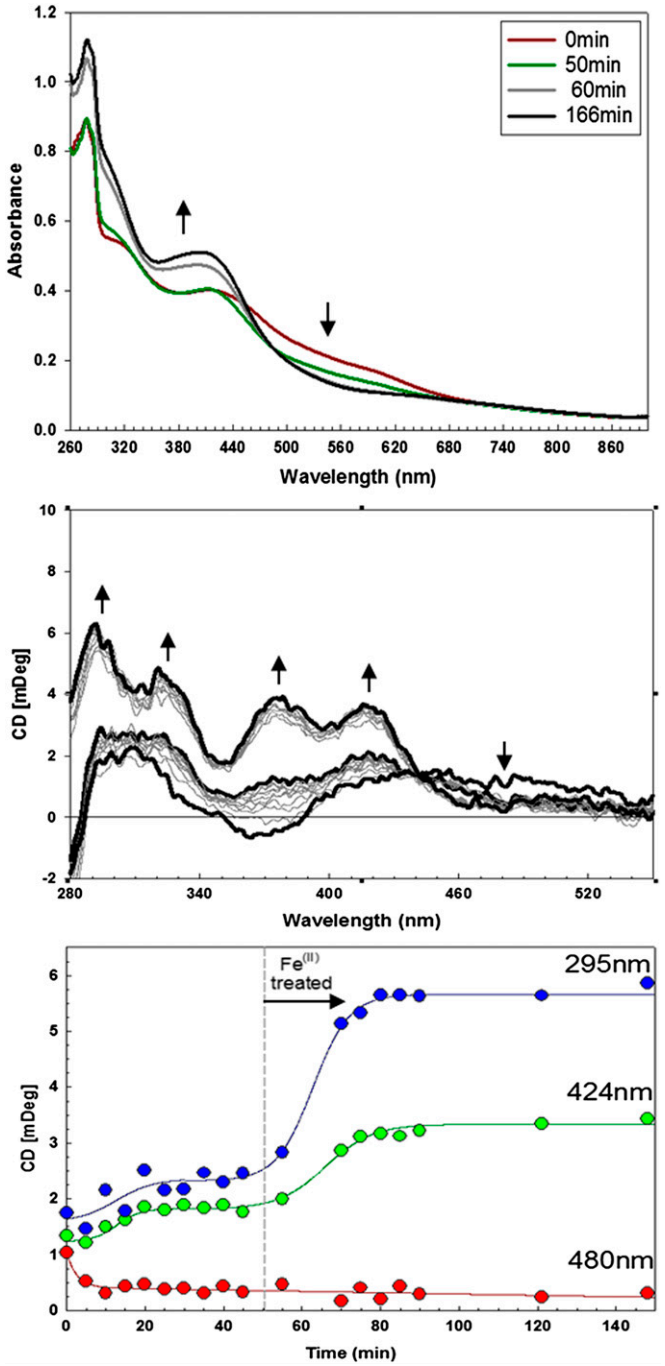

Fig. S4. UV-visible absorption and CD time course of $[2Fe\text{-}2S]^{2+}$ to $[4Fe\text{-}4S]^{2+}$ cluster conversion in FNR after repurification of $[2Fe\text{-}2S]^{2+}$-FNR. A sample of $[2Fe\text{-}2S]^{2+}$-FNR was obtained by exposing $[4Fe\text{-}4S]^{2+}$-FNR to O_2 for 2 min and repurified using a gel-filtration column (PD10; GE Healthcare). The concentration of $[2Fe\text{-}2S]^{2+}$ centers in FNR was 50 μM. The samples were treated with 3 mM DTT at 0 min and a fourfold excess of ferrous ammonium sulfate was added after 50 min under anaerobic conditions inside a glove box. (*Top*) Absorption spectra recorded after 0, 50, 60 and 166 min; arrows indicate the direction of change of absorption intensity as a function of time at discrete wavelengths. (*Middle*) CD spectra (gray lines) recorded between 0, 50 and 166 min (bold lines); arrows indicate the direction of change of CD intensity as a function of time at discrete wavelengths. (*Bottom*) Plot of CD intensity at 295, 424, and 480 nm as a function of time.

Table S1. Comparison of the resonance Raman Fe-S frequencies (cm^{-1}), assignments, and $^{32}S/^{34}S$-bridging isotope shifts (cm^{-1}) for $[4Fe\text{-}4S]^{2+}$ centers in a synthetic analog complex, *C. pasteurianum* ferredoxin, and *Escherichia coli* FNR

D_{2d} (T_d) Assignment	Solid cube*	Fd†	FNR
Mainly Fe-S(Cys) stretching			
A_1	391 (1)‡	395 (4)	392 (0)
$B_2(T_2)$	367 (1)	351 (1)	366 (0)
$E(T_2)$	359 (1)	363 (2)	354 (0)
Mainly Fe-S(bridging) stretching			
$B_2(T_2)$			
$E(T_2)$	385 (6)	380 (6)	392 (3)
A_1	335 (8)	338 (7)	335 (6)
$A_1(E)$	298 (5)	298 (5)	300 (3)
$B_1(E)$	283 (4)	276 (4)	286 (3)
$E(T_1)$	283 (4)		
$A_2(T_1)$	270 (3)	266 (4)	274 (2)
$B_2(T_2)$	249 (6)		
$E(T_2)$	243 (5)	251 (6)	254 (4)

*$(Et_4N)_2[Fe_4S_4(SCH_2Ph)_4]$ in KCl pellet at 77 K. Data from Czernuszewicz et al. (1).
†*C. pasteurianum* 8Fe ferredoxin as a frozen solution at 77 K. Data from Czernuszewicz et al. (1).
‡Numbers in parenthesis are downshifts on ^{34}S substitution of bridging S atoms, all values are ± 1 cm^{-1}.

1. Czernuszewicz RS, Macor KA, Johnson MK, Gewirth A, Spiro TG (1987) Vibrational mode structure and symmetry in proteins and analogues containing Fe_4S_4 clusters: Resonance Raman evidence for different degrees of distortion in HiPIP and ferredoxin. *J Am Chem Soc* 109:7178–7187.